Therapeutic Discovery

Molecular Cancer Therapeutics

Identification and Characterization of NVP-BKM120, an Orally Available Pan-Class I PI3-Kinase Inhibitor

Sauveur-Michel Maira[1], Sabina Pecchi[3], Alan Huang[4], Matthew Burger[3], Mark Knapp[3], Dario Sterker[1], Christian Schnell[1], Daniel Guthy[1], Tobi Nagel[3], Marion Wiesmann[1], Saskia Brachmann[1], Christine Fritsch[1], Marion Dorsch[1], Patrick Chène[1], Kevin Shoemaker[3], Alain De Pover[1], Daniel Menezes[3], Georg Martiny-Baron[2], Doriano Fabbro[2], Christopher J. Wilson[5], Robert Schlegel[4], Francesco Hofmann[1], Carlos García-Echeverría[1], William R. Sellers[6], and Charles F. Voliva[3]

Abstract

Following the discovery of NVP-BEZ235, our first dual pan-PI3K/mTOR clinical compound, we sought to identify additional phosphoinositide 3-kinase (PI3K) inhibitors from different chemical classes with a different selectivity profile. The key to achieve these objectives was to couple a structure-based design approach with intensive pharmacologic evaluation of selected compounds during the medicinal chemistry optimization process. Here, we report on the biologic characterization of the 2-morpholino pyrimidine derivative pan-PI3K inhibitor NVP-BKM120. This compound inhibits all four class I PI3K isoforms in biochemical assays with at least 50-fold selectivity against other protein kinases. The compound is also active against the most common somatic PI3Kα mutations but does not significantly inhibit the related class III (Vps34) and class IV (mTOR, DNA-PK) PI3K kinases. Consistent with its mechanism of action, NVP-BKM120 decreases the cellular levels of p-Akt in mechanistic models and relevant tumor cell lines, as well as downstream effectors in a concentration-dependent and pathway-specific manner. Tested in a panel of 353 cell lines, NVP-BKM120 exhibited preferential inhibition of tumor cells bearing PIK3CA mutations, in contrast to either KRAS or PTEN mutant models. NVP-BKM120 shows dose-dependent *in vivo* pharmacodynamic activity as measured by significant inhibition of p-Akt and tumor growth inhibition in mechanistic xenograft models. NVP-BKM120 behaves synergistically when combined with either targeted agents such as MEK or HER2 inhibitors or with cytotoxic agents such as docetaxel or temozolomide. The pharmacological, biologic, and preclinical safety profile of NVP-BKM120 supports its clinical development and the compound is undergoing phase II clinical trials in patients with cancer. *Mol Cancer Ther; 11(2); 317–28. ©2011 AACR.*

Introduction

Because of their crucial role in signal transduction, the dysregulated metabolism of phosphoinositides represents a key step in many disease settings. Multiple enzymes participate in the phosphorylation and dephosphorylation of the inositol head group of phosphoinositide lipids (1). Among them, the phosphoinositide 3-kinases (PI3K) have been the focus of extensive research and drug discovery activities for the last 20 years. Genetic alterations at multiple nodes in the PI3K pathway have been implicated in oncogenesis and cancer (2, 3). PI3K activation can occur in response to (i) constitutively active mutants and/or amplification of growth factor receptor tyrosine kinases (RTK) as in breast cancer with HER2 amplification (4), (ii) amplification of PI3K, (iii) gain of activating somatic mutations in the PIK3CA gene encoding the p110α catalytic subunit (5), (iv) overexpression or activating mutations of the downstream effector kinase Akt (6), (v) loss or inactivating mutations of PTEN (the phosphatase that breaks down phosphatidylinositol-(3,4,5)-trisphosphate (PIP3), or (vi) constitutive recruitment and activation by mutant forms of the Ras oncogene. Given this pervasive involvement in many cancers, the development of molecules that inhibit this pathway have recently been initiated in first in man studies (7).

Authors' Affiliations: [1]Oncology Disease Area, [2]Center for Proteomic Chemistry, Novartis Institutes for Biomedical Research, Basel, Switzerland; [3]Oncology Disease Area, Novartis Institutes for Biomedical Research, Emeryville, California; [4]Oncology Translational Medicine, BU Oncology, Novartis Pharma Inc.; [5]Developmental and Molecular Pathways, and [6]Oncology Disease Area, Novartis Institutes for Biomedical Research, Cambridge, Massachusetts

Note: Supplementary material for this article is available at Molecular Cancer Therapeutics Online (http://mct.aacrjournals.org/).

S.-M. Maira and S. Pecchi contributed equally to this work.

Current address for C. García-Echeverría: Oncology Drug Discovery and Preclinical Research, Sanofi-Aventis, Vitry-sur-Seine, France; and current address for M. Dorsch, Oncology Drug Discovery and Preclinical Research, Sanofi-Aventis, Cambridge, Massachusetts.

Corresponding Author: Sauveur-Michel Maira, Novartis Institute for Biomedical Research, Oncology Disease Area, Novartis Pharma AG, Klybeckstrasse 141, CH-4002 Basel, Switzerland. Phone: 41-61-69-67910; Fax: 41-61-69-65571; E-mail: sauveur-michel.maira@novartis.com

doi: 10.1158/1535-7163.MCT-11-0474

Following the discovery of NVP-BEZ235, our first dual pan-PI3K/mTOR clinical compound (8), we sought to identify additional PI3K inhibitors from different chemical classes with different profiles against targets within the PI3K pathway. Because the PI3K pathway is a complex signaling pathway composed of multiple and interconnected components, elucidation of effectiveness and tolerability of novel therapeutic modalities is likely to depend upon clinical experience with a number of clinical candidates with varying pathway profiles. An example of this pathway complexity is the regulation of the oncoprotein Akt. To be activated, Akt is first recruited to the plasma membrane through a direct interaction between its *N*-terminal pleckstrin homology domain and PIP3 molecules. For full activity, Akt is then phosphorylated on 2 distinct sites: on Thr308 by PDK1 and on Ser473 by the mTORC2 complex (9). Once activated, Akt regulates key downstream effectors, including the downregulation of mTORC1, the master regulator of protein translation, growth, and autophagy. However, genetic and biochemical studies have shown that mTORC1 provides a negative feedback loop at the level of RTKs causing reactivation of the PI3K and the mitogen-activated protein (MAP) pathway upon mTORC1 inhibition. The same negative feedback loop was showed in tumor biopsies from patients treated with the mTORC1 inhibitor RAD001 (10). Thus, in some but not all clinical contexts, the combined inhibition of both PI3K and mTOR might be necessary for effective therapy. Given that different wiring applies depending on the genetic alterations responsible for PI3K pathway constitutive activation (11, 12), compounds with varied and well understood profiles will be necessary to design and develop tailored chemotherapy.

Here, we report on the biologic characterization of the clinical candidate NVP-BKM120. This molecule is a 2,6-dimorpholino pyrimidine derivative that is a potent pan-PI3K inhibitor. Unlike NVP-BEZ235, it does not significantly inhibit mTOR and is highly selective against other protein or lipid kinases. NVP-BKM120 exhibits potent antiproliferative and proapoptotic activities in tumor cell lines by specifically blocking the biologic function of PI3K signaling components. NVP-BKM120 shows good oral bioavailability in mice and its on-target activity observed in cellular assays translates well in *in vivo* models of human cancer in which NVP-BKM120 shows significant tumor growth inhibition or regression at tolerated doses.

Materials and Methods

Compounds and tools

NVP-BKM120 was synthesized in the Global Discovery Chemistry group (NIBR Oncology; Novartis). NVP-BKM120, RAD001 (Novartis), STI571 (Novartis), Wortmannin (Alexis; #ALX-350–020-M001), LY294002 (Alexis; #ALX-270–038-M025), ZSTK474 (LC Laboratories; #Z-1006), AZD6244 (Selleck Chemicals; #S1008), and AZD8055 (Active Biochem; #A-1008) were prepared as 10 mmol/L stock (except LY294002; 20 mmol/L) solutions in 100% dimethyl sulfoxide (DMSO). Working solutions were freshly prepared before addition to the cell media such that final DMSO concentrations were kept constant at 0.1% in both control and compound-treated cells. Platelet-derived growth factor (PDGF) stock solution was prepared as recommended by the manufacturer (Sigma; #P4306).

In vitro kinase assays

PI3K assay. All the biochemical *in vitro* PI3K and protein kinase assays shown in Table 1 were previously described (13).

mTOR TR-FRET assay. Fifty nanoliters of compound dilutions were dispensed onto black 384-well low-volume nonbinding polystyrene plates (Corning; NBS#3676). Then 5 μL of ATP and GFP-4EBP1 with 5 μL mTOR proteins (final assay volume: 10 μL) were added, and the reaction was incubated at room temperature in 50 mmol/L HEPES pH 7.5, 10 mmol/L $MnCl_2$, 50 mmol/L NaCl, 1 mmol/L EGTA, and 1 mmol/L DTT. Reactions were stopped with 10 μL of a proprietary mixture (IVG), containing the Tb^{3+}-α-p4EBP1-(pT46) detection antibody, EDTA, in TR-FRET dilution buffer. Plates were then read 15 minutes later in a Synergy 2 reader using an integration time of 0.2 second and a delay of 0.1 second. The control for 100% inhibition of the kinase reaction was created by replacing the mTOR kinase with an equal volume of reaction buffer. The control for 0% inhibition was created by substituting solvent vehicle (90% DMSO in H_2O) without added test compounds. The TR-FRET mTOR kinase assay components were purchased from Invitrogen Corporation. Details are available upon request.

DNA-dependent protein kinase assay. To determine the potency of NVP-BKM120 on the phosphatidylinositol 3-kinase–related kinases (PIKK) family member DNA-PK, an *in vitro* assay kit from Promega (SignaTECT; # V7870) was used in combination with the purified DNA-PK enzyme from Promega [DNA-dependent protein kinase (DNA-PK), V5811]. The *in vitro* kinase assay reactions were conducted according to the manufacturer's protocol but modified as follows: 27 U of purified DNA-PK protein/reaction, 1 μmol/L ATP/reaction, 1% DMSO, or indicated compound/reaction at 37°C for 30 minutes.

PI3Kα kinetic studies. PI3Kα was incubated for 60 minutes in coated Maxisorp plates (14) in 50 μL medium containing [γ^{33}P]-ATP (~6 kBq/well), 0.5 to 400 μmol/L unlabelled ATP, 5 mmol/L $MgCl_2$, 150 mmol/L NaCl, 25 mmol/L Tris-HCl pH 7.4, and 1% DMSO. The reaction was started by adding PI3Kα (0.4 μg/mL) and stopped by adding 50 μL of 50 mmol/L EDTA. Plates were washed twice with Tris-HCl buffer and dried, after which 100 μL/well MicroScint PS was added and bound radioactivity was determined using a TopCount (Packard) counter. Curves were fitted to a mixed inhibition model (15) by nonlinear 3 dimensional regression. In this model,

Table 1. Biochemical profile of NVP-BKM120 against selected protein kinases, class I and IV PI3Ks, and PI4Kβ

Enzyme	IC_{50}, nmol/L	Enzyme	IC_{50}, nmol/L
Class I PI3Ks[a]			
p110α	k52 ± 37 ($n = 7$)	p110β	166 ± 29 ($n = 3$)
p110α-H1047R	58 ± 2 ($n = 2$)	p110δ	116 ($n = 1$)
p110α-E545K	99 ± 6 ($n = 2$)	p110γ	262 ± 94 ($n = 7$)
Class III			
Vps34[b]	2,410 ± 150 ($n = 19$)		
Class IV PI3Ks			
mTOR[c]	2,866 ± 1,671	DNA-PK[a]	>10,000
ATR[d]	8,091 ± 2,038		
PI4K			
PI4Kβ[b]	>25,000 ($n = 22$)		
Protein kinases			
Axl	>10,000	Fak	>10,000
VEGFR2/Kdr	>10,000	Jak2	>10,000
HER1/ErbB1	>10,000	c-Abl	>10,000
IGF1-R	>10,000	c-Src	>10,000
EphB4	>10,000	PKA	>10,000
Ret	>10,000	Akt1/PKBα	>10,000
Tie-2/Tek	>10,000	PDK1	>10,000
c-Met	>10,000	$B\text{-}Raf^{V599E}$	9,200
K650E-FGFR-	>10,000	CDK2/cyclin A	>10,000
CSF1R	582		

NOTE: *In vitro* kinase assays were conducted with the indicated recombinant PI3K lipid or protein kinases, in the presence of increasing concentrations of NVP-BKM120, as described in Materials and Methods. The concentration responsible for 50% inhibition of the activity is reported (IC_{50}) in nmol/L as determined in multiple experiments (n) is shown as an average ± one SD.
[a]Filter binding assay format.
[b]Kinase-Glo format.
[c]TR-FRET assay format.
[d]Alpha Screen assay format.

the enzyme activity is related to S (ATP) and I (NVP-BKM120) by the following equation:

$$v = \frac{V_{max} \times [S]}{K_1 \times (1 + [I]/K_2) + [S] \times (1 + [I]/K_3)},$$

in which the apparent dissociation constant of ATP is represented by K_1 and the apparent dissociation constants of the inhibitor are represented by K_2 (competitive component) and K_3 (noncompetitive component).

Cellular biology

Cell lines and cell culture: Mechanistic models. To evaluate the isoform-specific potency of NVP-BKM120 in a cell-based system, an *N*-terminally myristoylated form of each PI3K class IA isoform was expressed in Rat1 fibroblasts. The retroviral expression plasmid pBabePuro (16) containing human p110α, p110β, and p110δ with an *N*-terminal myristoylation (myr) signal followed by an HA-tag were generated as described (17). Successfully infected Rat1 cells were selected in medium containing 4 μg/mL of puromycin, expanded and characterized for expression of the p110 isoforms. Transgenic expression of the myristoylated protein was confirmed by increased levels of phosphorylated Akt. The $TSC1^{-}/^{-}$-null MEFs mechanistic model for mTORC1 constitutive activation are from Dr. D. Kwiatkowski (Brigham & Women's Hospital, Boston, MA; ref. 18).

Cell lines and cell culture: Human tumor cell lines. The culture conditions used to maintain U87MG, SF268, HT-29, PC3M, HCT116, and BT474 are described elsewhere (8, 19). The U87MG (University of Basel, Basel, Switzerland), HCT116 (American Type Culture Collection; #CCL-247), and BT-474 (Friedrich Miescher, Institute, Basel, Switzerland) cell lines were authenticated by single-nucleotide polymorphism analysis. The SF268 cell line (National Cancer Institute, Bethesda, MD) was not authenticated.

Biochemical characterization upon compound exposure and antibodies. A total of 2×10^6 cells were seeded per 10-cm dish. Eighteen hours later, the medium was discarded and replaced with 10 mL of fresh medium

containing the test items. Unless specified in the figure legend, the incubation period was 30 minutes. For agonist activation, cells were first starved for 18 hours in 9 mL of medium containing only 0.05% FBS. Then cells were pretreated for 30 minutes by addition of 1 mL of medium containing the test items and subsequently stimulated for 10 minutes with the agonist (final concentrations: 50 ng/mL for PDGF, 100 ng/mL for epidermal growth factor (EGF), 60 ng/mL interleukin (IL)-4, and 1 μmol/L anisomycin). Cells were washed twice, lysed, and processed by Western blot analysis as described (8).

S473P- and T308P-Akt ELISA assays; S473P-Akt and S235/236P-RPS6 RPPA quantification. All the procedures have been described elsewhere (8, 20).

In vivo studies

Compound preparation. NVP-BKM120 and AZD6244 were formulated in NMP/PEG300 (10/90, v/v). Solutions were freshly prepared for each day of dosing by dissolving the powder, first in *N*-Methyl-2-pyrrolidone (NMP) with sonication and then by adding the remaining volume of PEG300. The application volume was 10 mL/kg. Herceptin/trastuzumab (150 mg; Hammer Apotheke) was prepared as a 0.22 μmol/L filtered sterile stock solution at 15 mg/mL in PBS that was subsequently diluted to 1 mg/mL aliquots and stored at −80°C. For each treatment (3 times per week), a new vial was thawed for immediate intraperitoneal treatment in animals with an application volume of 10 mL/kg (final dose of 10 mg/kg).

In life experimentation and efficacy studies. A maximum of 10 female Harlan nude (HsdNpa:Athymic Nude-*nu*) mice (8–10 weeks of age) were kept under sterile conditions (type III cage, in an Optimal Hygienic Conditions zone) with free access to food and water. Subcutaneous tumors were established by injection of 100 μL of PBS containing 2×10^6 tumor cells (Rat1-myr-p110α, U87MG, HCT116, NCI-N87, and PC3M), in left flank of each animal. Orthotopic BT-474 tumors were established by injection of 5×10^6 cells prepared in 30% Hank's Balanced Salt Solution (HBSS) containing 10% Matrigel, in the third mammary gland. Treatments were initiated when the mean tumor volume in each randomized group ($n = 6$–8) reached 100 to 150 mm^3. For BKM120, treatments were carried out orally, once per day, using an application volume of 10 mL/kg. Treatments were stopped and animals sacrificed when the tumor size in the vehicle control group reached 1,000 to 1,200 mm^3. Tumor volumes were determined by using calipers for measurement of longest (considered as length) and shortest (considered as diameter) dimensions of each tumor and according to the formula length × $diameter^2$ × π/6. Antitumor activity is expressed as T/C% (mean increase of tumor volumes of treated animals divided by the mean increase of tumor volumes of control animals multiplied by 100). Data are presented as means ± one SEM. Comparisons between groups and vehicle control group were done using either one-way ANOVA or ANOVA on ranks followed by the Dunnett tests when data were, respectively, either normally distributed or not. For all tests, the level of significance was set at $P < 0.05$. Calculations were carried out with SigmaStat v 2.03 (Jandel Scientific). All experimental procedures (approved by the Kantonales Veterinäramt Basel-Stadt under license #1769) strictly adhered to the Eidgenössisches Tierschutzgesetz and the Eidgenössische Tierschutzverordnung. For combination *in vivo* studies, the combination was determined using the Clarke method (21).

NVP-BKM120 tissue analytics, interstitial fluid pressure, and DCE-MRI. The methodologies used were as described previously (22).

Results

NVP-BKM120: chemical structure and mechanism of action

NVP-BKM120 (Fig. 1A) was identified upon optimization of drug-like and *in vivo* protein kinase properties from a 2-morpholino-6-aminopyridyl-pyrimidine scaffold. The molecule binds in the ATP-binding site of the lipid kinase domain, as determined from its cocrystal structure in the PI3K p110γ isoform (PDB accession code: 3SD5) and by homology modeling in the PI3K p110α isoform (Fig. 1B). The alpha model suggests that there are 3 key hydrogen bond interactions (indicated by the dotted lines), formed by the oxygen of the 2-morpholino group and by the exocyclic nitrogen in the 6-position pyridyl substituent. The morpholine oxygen functions as a hydrogen bond acceptor with the backbone amino group of Val^{851} in the hinge domain of the PI3K p110α isoform. A similar interaction is observed in all the published structures with ATP and with known inhibitors (23, 24). The 6-pyridyl exocyclic nitrogen (as a donor) binds to Asp^{810} and Asp^{933} in the catalytic region. A fourth interaction could be modeled, as high resolution structures of p110γ are frequently observed to contain a water molecule forming a hydrogen bond bridge between Tyr^{836} and Asp^{810} (25). Its presence could provide an additional hydrogen bond formed by its interaction with the 6-pyridyl endocyclic nitrogen acting as an acceptor.

Kinetic fittings of enzymatic results using a Michaelis–Menten model revealed that NVP-BKM120 inhibits PI3Kα via a mixed-type mode (15), affecting both the V_{max} and the K_m for ATP (Fig. 1C). Because the K_m for ATP increases with compound concentration (and correspondingly, the compound IC_{50} value increases with ATP competition), NVP-BKM120 has greater affinity for the free, relative to the ATP bound, PI3K enzyme. While further study of the ATP-noncompetitive aspect has not been yet pursued, the ATP-competitive facet of this inhibition is consistent with the binding mode established by the crystallography results described earlier.

Biochemical selectivity of NVP-BKM120

NVP-BKM120 is approximately equipotent against the class IA PI3Ks α, β, and δ and modestly less potent against the class IB γ isoform (Table 1). The compound also shows comparable potency against activating

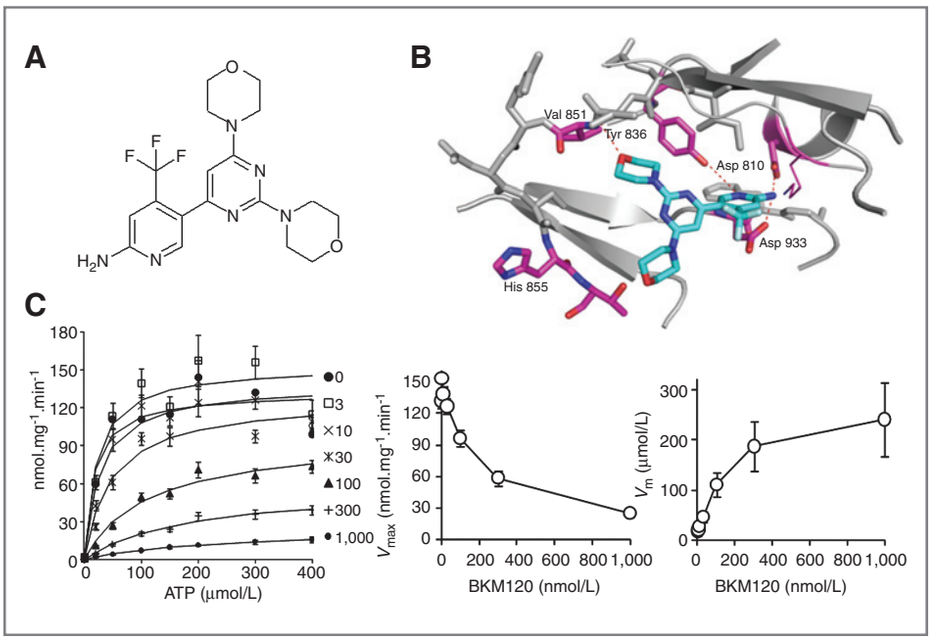

Figure 1. NVP-BKM120: structure, binding mode, and mechanism of action. A, chemical structure of NVP-BKM120. B, the proposed binding mode of NVP-BKM120 in the class 1A PI3K p110α isoform is shown. The PI3K p110α homology model was built with the Molecular Operating Environment software from the Chemical Computing Group using default settings in the alignment and homology modeling modules, a Novartis structure of NVP-BKM120 bound to PI3K p110γ (PDB deposition code: 3SD5) as a template and the input sequence of PI3K p110α (UNIPROT:P42336). All key protein–compound interactions were retained between the p110γ structure and the p110α model, and no new interactions were expected with the other PI3K class I isoforms. C, PI3K p110α kinetic reactions in presence of NVP-BKM120 were done as described in Materials and Methods. NVP-BKM120 concentrations (nmol/L) were as indicated in the graph. Curves were fitted to a mixed inhibition model by nonlinear 3 dimensional regression. The predicted V_{max} and K_m are plotted on the right top and bottom, respectively. The mixed model was highly significant as compared with the competition model in a global fit ($P < 0.001$). The predicted V_{max} and K_m calculated with the equations $V_{max}^{app} = \frac{V_{max}}{1+[I]/K_3}$ and $K_m^{app} = K_1 \times \frac{1+[I]/K_2}{1+[I]/K_3}$ are plotted in the right top and bottom, respectively. Points on the right represent these parameters (± SE) calculated with the Michaelis–Menten equation by nonlinear 2 dimensional regression.

p110α somatic mutations that have been described in a wide array of human cancers (26). NVP-BKM120 is significantly less potent in biochemical assays against the PI3K class III family member Vps34, the related class IV PIKK protein kinases mTOR, ATR, and DNA-PK, and the distinct lipid kinase PI4Kβ. NVP-BKM120 was shown to be mostly inactive against all the kinases tested in an in-house selectivity panel with the exception of colony-stimulating factor 1 receptor (CSF1R). This inhibitory activity was confirmed at a concentration of 5 μmol/L in the Invitrogen functional kinase panel Supplementary Table S1 but no effect was observed in a cell-based CSF1R autophosphorylation assay (Supplementary Fig. S1A). NVP-BKM120 was further profiled in the Ambit kinase competition panel (Supplementary Table S2), in which EphA2 and fibroblast growth factor receptor 2 (FGFR2) kinases were found to be inhibited by more than 90% at a concentration of 1 μmol/L. Such as for CSF1R, these hits were not reconfirmed in FGFR2 (Supplementary Fig. S1B) and EphA2 (Supplementary Fig. S1C) cellular autophosphorylation assays. Therefore, NVP-BKM120 can be considered as a selective pan-class I PI3K inhibitor with a profile distinct from the previously described dual PI3K/mTOR inhibitor NVP-BEZ235 (8).

Activity and specificity of NVP-BKM120 in cell systems

Rat1 cell lines that overexpress activated versions of each class IA PI3K isoform were engineered and pathway activation was confirmed by the concomitant increase in S473P-Akt levels (Supplementary Fig. S2). NVP-BKM120 inhibited S473P-Akt in a concentration-dependent manner (Fig. 2A) with IC_{50} values (RPPA determination) of 104 ± 18, 234 ± 47, and 463 ± 87 nmol/L ($n = 7$) in lines that express myr-p110α, β, and δ, respectively. These reductions in S473P-Akt levels are probably not attributable to mTOR inhibition, as the IC_{50} value for S6RP S235/236 phospho levels was 922 ± 142 nmol/L ($n = 5$) in the mTORC1 constitutively activated $TSC1^{-/-}$ cells. In contrast, the dual PI3K/mTOR NVP-BEZ235 as well as the mTOR catalytic inhibitor AZD8055 (27) and NVP-BEZ235 were, as expected, extremely active in this assay with IC_{50} values of 3.5 ± 0.6 ($n = 4$) and 2.0 ± 0.8 ($n = 4$), respectively (Fig. 2B).

In PTEN-null U87MG cells, NVP-BKM120 treatment reduced both S473P-Akt (IC_{50} value: 130 ± 44 nmol/L, ELISA) and T308P-Akt (IC_{50} value: 229 ± 40 nmol/L, ELISA) levels with similar potency comparable with what is observed in the mechanistic Rat1-myr-p110

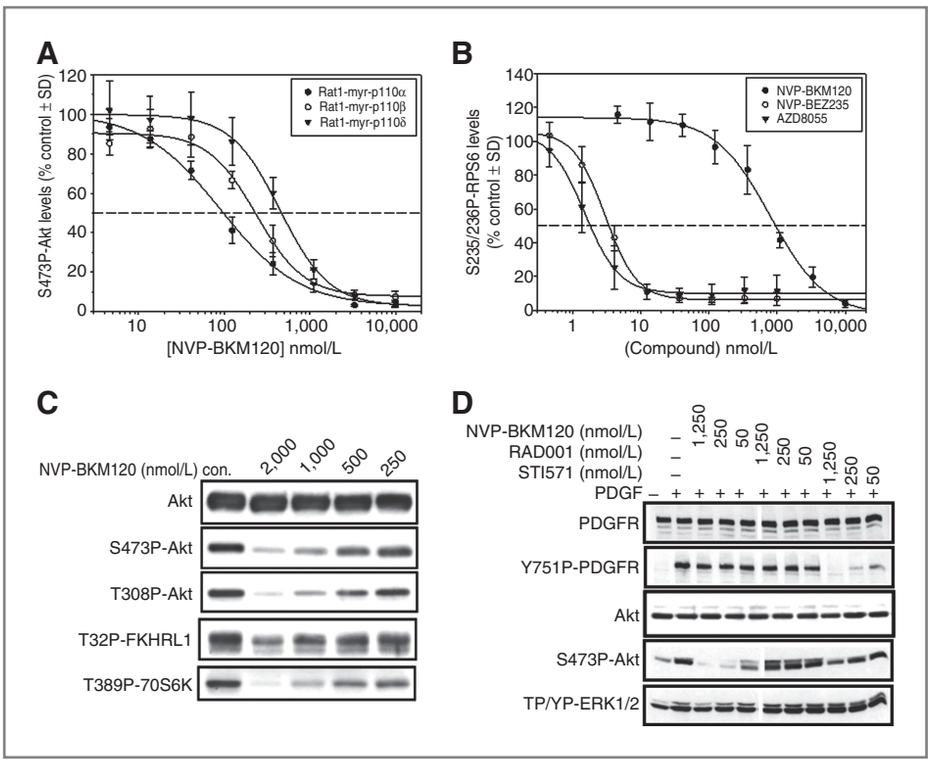

Figure 2. NVP-BKM120 efficiently and specifically inhibits PI3K in mechanistic and disease cell-based models. A and B, Rat1-myr-p110α, β, and δ (A) and TSC1$^{-/-}$-null MEFs (B) cell lines were incubated for 30 minutes with the indicated compound and concentrations (in nmol/L). Cells were then lysed and analyzed by RPPA for their S473P-Akt and S235/236P-RPS6 levels. Levels were then plotted as percentage of untreated control cells and IC_{50} values determined. C, U87MG cells were exposed for 30 minutes to the indicated amount of NVP-BKM120 and cell extracts subsequently analyzed by Western blotting for the indicated PI3K pathway markers. D, SF268 cells were starved for 18 hours, pretreated for 30 minutes with 50, 250, or 1,250 nmol/L of the indicated compounds and then stimulated with PDGF for 10 minutes. Cells were then lysed and cell extracts analyzed by Western blotting for the indicated markers.

models (Fig. 2C). This effect is correlated in a dose-dependent manner with inhibition of downstream direct (FOXO3A/FKHRL1) and indirect (p70S6K) Akt effectors, showing profound Akt pathway modulation upon NVP-BKM120 exposure. Compound washout studies in U87MG cells showed that these inhibitory effects are fully and rapidly reversible upon compound withdrawal (Supplementary Fig. S3), suggesting rapid binding kinetics and a short residence time of the compound on the target.

To further evaluate the specificity of NVP-BKM120, the compound was tested in cellular models in the presence of various agonists that activate a spectrum of well-characterized signaling pathways. In the presence of mitogenic stimuli such as PDGF (Fig. 2D) or EGF (Supplementary Fig. S4A), NVP-BKM120 blocked S473P-Akt induction by the respective growth factors but failed to affect receptor activation (Y751P-PDGFR and Y845P-EGFR, respectively) and activation of the mitogen-activated protein kinase (MAPK) pathway. This is in contrast to the effects observed with PDGF receptor (STI571) or EGF receptor (NVP-AEE788) inhibitors. Similarly, NVP-BKM120 did not inhibit IL-4–induced activation of STAT6 (Supplementary Fig. S4B), anisomycin-induced activation of c-*jun*-NH_2-kinase (JNK) and p38 (Supplementary Fig. S4C) nor class IV PIKK (ATM and DNA-PK) activation in response to DNA double-strand breaks (Supplementary Fig. S4D). Cumulatively, these results further show the specificity of NVP-BKM120 in a cellular context.

NVP-BKM120 shows preferential inhibition of tumor cells bearing oncogenic mutations in the PIK3CA gene

Activation of the PI3K pathway is a common feature in human cancers, arising through various genetic abnormalities (28). To test whether NVP-BKM120 would be an effective treatment for tumors presenting these abnormalities, the antiproliferative activity of the molecule was determined against a panel of 353 cell lines that vary with respect to key genetic determinants such as the status of the *PIK3CA*, *PTEN*, and *KRAS* genes. Cell lines characterized by the presence of an oncogenic mutation in the PIK3CA gene showed greater and statistically significant ($P = 0.01$) sensitivity to NVP-BKM120 than cells bearing a nonmutated wild-type form of the gene (Fig. 3A). No differences in sensitivity could be observed when comparing cells carrying a deletion or a mutation in the *PTEN* gene (Fig. 3B) or an activating mutation in the *KRAS* gene (Fig. 3C) when compared with cells bearing wild-type *PTEN* and *KRAS* genes, respectively. However, in the latter case, a trend toward more sensitivity in KRAS wild-type cells is seen. PIK3CA and KRAS mutation often co-occur in human colorectal adenocarcinoma. A multivariate analysis looking at status of both genes revealed that PIK3CA mutant/KRAS wild-type tumors are most sensitive to NVP-BKM120 versus other possible combinations (Supplementary Fig. S5A) and most notably in comparison to PIK3CA mutant/KRAS mutant models ($P = 0.00005$). These data show that the presence of a KRAS mutation could overcome the sensitivity to a PI3K

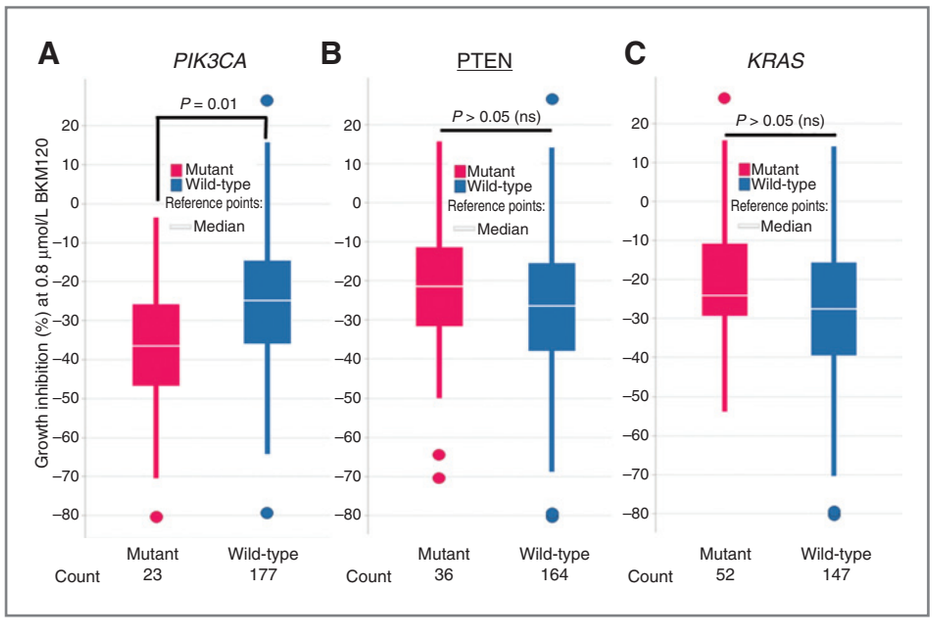

Figure 3. NVP-BKM120 preferentially inhibits the proliferation of tumor cells with *PIK3CA* gene-bearing oncogenic mutations. Cell lines with different genetic lesions were binned and the percentages of growth inhibition with treatment at 0.8 μmol/L of NVP-BKM120 were plotted as box plots and compared between 23 PIK3CA mutant cancer cell lines and 177 PIK3CA WT cell lines (A), 36 PTEN mutant cell lines and 164 PTEN wild-type cell lines (B), and 52 KRAS mutant cell lines and 147 KRAS wild-type cell lines (C). *P* values were determined by the Student *t* test; medians of the group are labeled on each plot as the white bars.

inhibitor, probably by activation of alternate, KRAS-dependent signaling pathways such as the extracellular signal-regulated kinase (ERK) pathway. Interestingly, cotreatment of NVP-BKM120 with a MAP/ERK kinase (MEK) inhibitor could induce cell death, as revealed by PARP cleavage, in KRAS mutant/PIK3CA mutant HCT116 cells when single-agent treatment was essentially ineffective (Supplementary Fig. S5B). A similar observation was made for ZSTK474, another pan-PI3K inhibitor (29), suggesting that this phenomenon is not unique to NVP-BKM120.

NVP-BKM120 efficiently inhibits the PI3K pathway in tumor-bearing animals and displays strong antitumor activity *in vivo*

To determine whether NVP-BKM120 could reach exposure leading to pathway modulation in tumor tissue, Rat1-myr-p110α tumor-bearing animals were treated orally, once, at dose levels of either 30 or 60 mg/kg. Phosphorylated Akt levels (Ser 473) as well as compound concentrations were then determined, at different time points postdrug administration (Fig. 4A). Maximum inhibition of p-Akt levels in tumor tissue was achieved at the 1 hour time point when the concentration in both tumor and plasma compartments was highest, for both dose levels. Phosphorylated Akt levels remained strongly inhibited 8 hours postdose (the inhibition was equal or superior to 80%, at 30 and 60 mg/kg, respectively) and at 16 hours postdose for the 60 mg/kg dose level (70% inhibition). A similar relationship is observed in the PTEN-null U87MG model (Supplementary Fig. S6A). Overall, these data show that NVP-BKM120 oral administration can achieve pharmacodynamic effect in the tumor in a concentration-dependent manner, showing pharmacokinetic and pharmacodynamic relationship.

To show that the observed pharmacodynamic effects could translate into effective antitumor activity, Rat1-myr-p110α tumor-bearing mice were treated orally with NVP-BKM120 once per day at doses of 40, 50, or 60 mg/kg. At these dose levels, the compound was well tolerated (right) and a robust reduction in tumor mass (left) was observed (T/C values of −25%, −48%, and −46%, respectively; Fig. 4B), showing the ability of NVP-BKM120 to treat PI3K-addicted tumors. A similar response was observed in the MCF7 PIK3CA mutant model MCF7 (Supplementary Fig. S6C). Consistent with the *in vitro* data (Fig. 3), the compound was less efficacious against U87MG PTEN-null tumors in mice compared with PIK3A-mutated cell lines, even at the dose of 60 mg/kg (Supplementary Fig. S6B).

Because clinical benefit in the treatment of solid tumors is often obtained as a combination therapy, NVP-BKM120 was combined with a number of standards of care agents or with targeted inhibitors to model rational combinatorial treatments. Genetically engineered lung KRAS mutant tumors have been shown to be almost insensitive to PI3K inhibitor treatment, but complete efficacy was obtained when combined with a MEK inhibitor (30). Similarly, when grown *in vivo*, KRAS mutant/PIK3CA mutant HCT116 tumors were found to be relatively insensitive to suboptimal dose levels of either NVP-BKM120 or the MEK inhibitor AZD6244. However, significant tumor regression was observed in a very well-tolerated manner when both drugs were combined (Fig. 4C and Supplementary Fig. S6D). These data show that the combination of both drugs lead to activity superior to that seen with either agent alone. In agreement with this, more apoptosis was observed *in vitro*, when HCT116 were exposed to both drugs (Supplementary Fig. S5B).

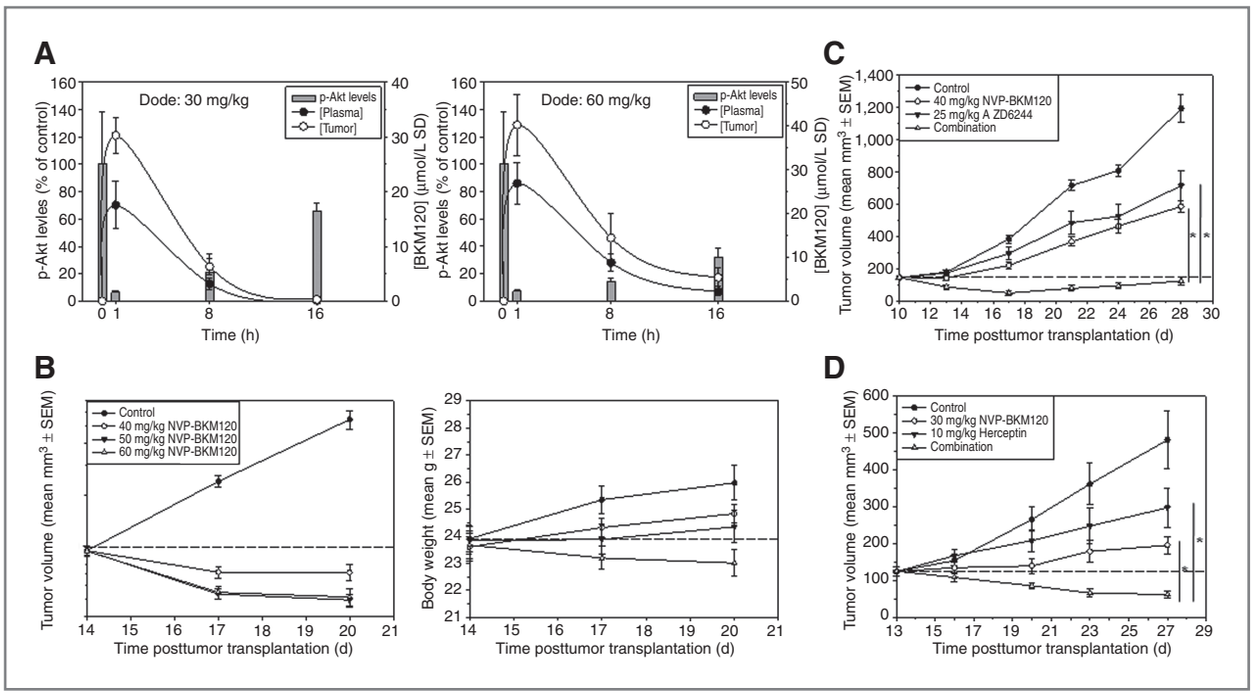

Figure 4. NVP-BKM120 pharmacokinetic/pharmacodynamic relationship and *in vivo* antitumor activities as a single agent or in combination. A, Rat1-myr-p110α tumor-bearing animals received a 30 mg/kg (left) or 60 mg/kg (right) oral acute treatment of NVP-BKM120. At the allotted times, the groups of mice ($n = 3$) were sacrificed and blood and tumor tissue were harvested and prepared for NVP-BKM120 concentration (by mass spectrometry analytics; right scale) and S473P-Akt levels determination (by RPPA, left scale). B–D, Rat1-myr-p110α (B), HCT116 (C), or BT474 (D) cells were grown as subcutaneous (B and C) or mammary fat pad orthotopic (D) xenografts in Harlan nude mice. Antitumor therapy studies ($n = 7$–8) with the indicated compounds were then started when the tumors reached a size of 100 to 150 mm^3 in average. NVP-BKM120 (B–D) and AZD6244 (C) were given orally once per day, whereas Herceptin was given 3 times per week through the intraperitoneal route (D). The changes over time in tumor volume are shown. The combination index (CI) as determined by the Clarke method (21) is: −0.25 (C) and −0.27 (D), respectively. Negative CI values are reflective of *in vivo* synergism.
*, $P < 0.05$ (Holm–Sidak).

As true for other pathways, the PI3K/Akt/mTORC1 pathway is subjected to regulation by negative feedback loops. Efficacy of PI3K inhibitors might, therefore, be limited by reactivation of critical upstream nodes. Such a phenomenon has recently been described in RTK-addicted tumor lines such as breast HER2-amplified models, in which PI3K inhibition led to ERK and PI3K pathway reactivation through HER2/HER3 overexpression and overactivation (31–34). Cotreatment with both PI3K and RTK inhibitors in RTK-addicted tumors is, therefore, warranted to avoid this adaptive mechanism of resistance. To test this hypothesis, orthotopic breast HER2-amplified BT474 tumor-bearing mice were treated with NVP-BKM120 in presence or absence of the HER2 antagonist trastuzumab (Fig. 4D and Supplementary Fig. S6E). Only partial responses could be obtained as single agents (T/C of 49.7% and 18.7% for Herceptin and BKM120, respectively) but significant tumor regression was obtained when both drugs were combined (T/C of −15%) with no impact on body weight. Similar data were obtained for the HER2-amplified gastric cancer tumor model NCI-N87 (Supplementary Fig. S7A).

The alkylating agent temozolomide or the microtubule stabilizer taxotere are 2 standard of care agents used to treat glioblastoma multiforme (GBM) or prostate cancer, respectively. In both indications, the PTEN gene is frequently inactivated, suggesting some dependencies on the PI3K signaling. Suboptimal dosage regimen of NVP-BKM120 (30 mg/kg) was used to check whether it could give advantages in combination studies to these agents. Whereas only partial activity is observed as single agent (as was the single agent use of temozolamide or taxotere), the combination of temozolamide or taxotere with NVP-BKM120 against GBM U87MG (Supplementary Fig. S7B) and prostate PC3M (Supplementary Fig. S7C) tumors, respectively, caused robust tumor shrinkage in a well-tolerated manner. These results show the potential for at least additive activities with these cytotoxic agents and NVP-BKM120 in selected settings.

Overall, these *in vivo* efficacy data show that NVP-BKM120 is an orally available PI3K inhibitor that displays a good correlation between its pharmacokinetic and specific pharmacodynamic readouts, resulting in a strong antitumor activity either alone or in combination with targeted or cytotoxic therapies in relevant disease models.

NVP-BKM120 possesses antiangiogenic activities *in vivo*

PI3K can be actively recruited and activated by angiogenic factors (35, 36). PI3K inhibitors are, therefore,

expected to display some degree of antiangiogenic activity. As described for NVP-BEZ235 (22), NVP-BKM120 treatment readily blocks VEGF induced neovascularization *in vivo* (Supplementary Fig. S8A). Angiogenic tumors are characterized by tortuous, chaotic, and highly permeable vessels. This phenomenon is in part due to VEGF-induced eNOS activation, through a PI3K-dependent mechanism involving Akt (22). Treatment of highly angiogenic rat mammary BN472 tumor-bearing rats with NVP-BKM120 led to significant reduction of tumor vasculature leakiness from the tumor tissue, as reflected by the strong reduction of Evans blue–mediated fluorescence (Supplementary Fig. S8B). As a consequence, NVP-BKM120 treatment also produced a strong reduction in tumor interstitial fluid pressure (IFP), which depends on the vasculature permeability (Fig. 5A). Reduction in permeability and IFP could be measured in a noninvasive manner by dynamic contrast enhanced (DCE)-MRI, in the presence of the contrasting agent Vistarem. Treatment of BN472 tumor-bearing rats with NVP-BKM120 strongly reduced tumor permeability as reflected by the rapid drop in K_{trans} factor (Fig. 5B). These data confirm that NVP-BKM120 possesses strong antiangiogenic properties and these can be visualized and quantified by DCE-MRI imaging technology.

Discussion

A plethora of preclinical evidence predicts that inhibitors targeting various components of the PI3K pathway will have therapeutic benefit in cancer. However, a key question that remains to be answered is: what is the most effective and tolerated inhibitory profile of a small molecule cancer therapeutic targeting this pathway? Because cancer is not one disease, but many, it is unlikely that all tumor types, encompassing different lineages and genetic status, would be similarly "wired" in this signal transduction machinery. Therefore, to maximize chances of clinical success, following the discovery of the dual PI3K/mTOR inhibitor and imidazoquinoline derivative NVP-BEZ235, we pursued the development of other clinical candidates from a different chemical space and with a different biologic profile.

This effort led to the discovery of NVP-BKM120, identified from the pan-PI3K inhibitor lead series 2-morpholino-4-amino-6-pyrimidinyl pyrimidines (MAPP) through a combination of structure-based drug design and optimization of *in vivo* properties (37). NVP-BKM120 inhibits PI3K in an ATP competitive manner, but this is the result of a mixed effect on K_m and V_{max}. NVP-BKM120 spares tyrosine or serine/threonine protein kinases, and unlike NVP-BEZ235, is not an effective mTOR inhibitor.

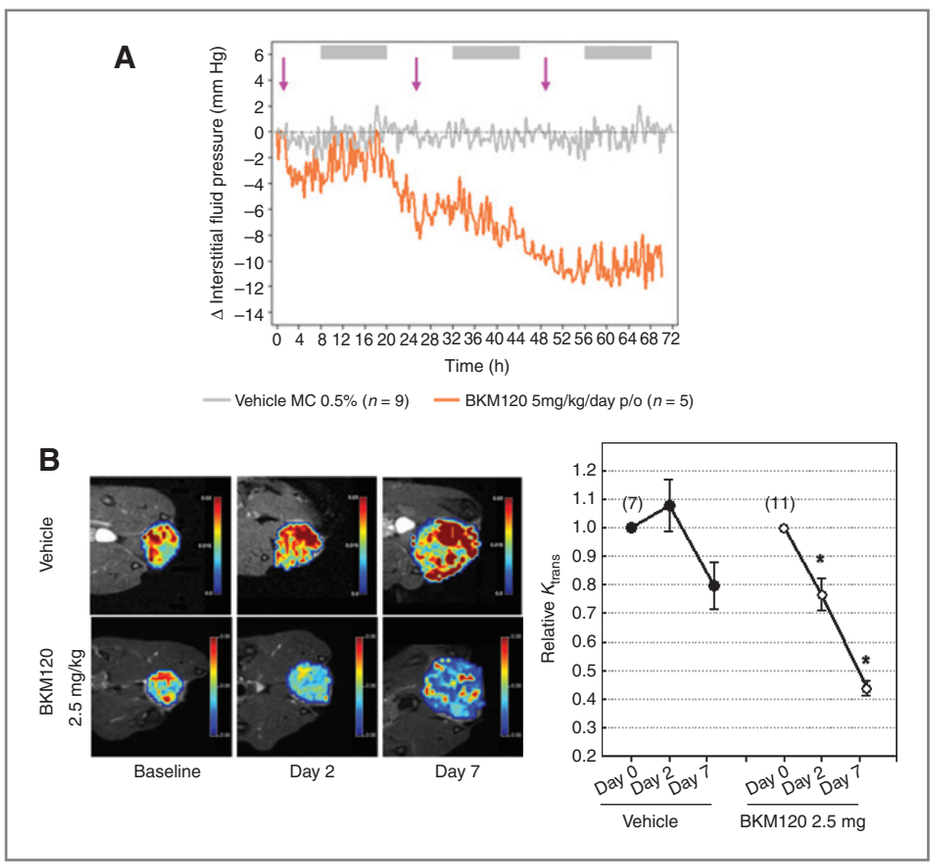

Figure 5. NVP-BKM120 reduces vasculature permeability and IFP in tumors. A, orthotopic BN472 tumor-bearing rats containing a pressure sensing catheter inserted in the tumor were treated for 3 consecutive days with NVP-BKM210 at 5 mg/kg ($n = 5$; initial IFP: 20.4 ± 2.6 mm Hg) or with the vehicle control ($n = 9$; 18.2 ± 1.5 mm Hg). The IFP was continuously recorded for 72 hours and variations (Δ toward initial values) plotted (gray lines, untreated animals; orange line, applied treatment as indicated in the graph). Data presented are means ± SEM. The arrows represent the administration schedule. Gray bars represent night time. B, quantitative evaluation on normalized K_{trans} (right) and K_{trans} maps (left) in BN472 tumors at days 0, 2, and 7 following once daily treatment with vehicle and BKM120 at 2.5 mg/kg.

This distinction can be explained by the binding modes of the 2 molecules: the proposed binding mode of NVP-BEZ235 in PI3Kα showed a key interaction with the Ser 774 residue of PI3K that was proposed to also be important for mTOR inhibition, due to the H-bond interaction with the mTOR corresponding residue, Ser 2665 (8). NVP-BKM120, on the other hand, lacks this contact with the Ser 774 residue providing a rationale why it is a much less effective mTOR inhibitor.

The effects of NVP-BKM120 on the PI3K pathway downstream biomarkers p-Akt and pRPS6 in mechanistic PI3K (Rat1-transduced cells) and mTORC1 ($TSC1^{-/-}$ minus MEFs) cell systems, respectively, show the predictability of the biochemical profile in a cellular environment. These effects were also observed in disease models, showing the potency, specificity, as well as the dose dependency of the compound to block the PI3K pathway in relevant cell-based models. NVP-BKM120 inhibitory effects in cells can be rapidly reverted upon drug washout, in agreement with the fast kinetics of the drug on PI3K observed *in vitro*. Pathway inhibition by NVP-BKM120 led to proliferation inhibition in a variety of cell lines, representing different lineages and genetic abnormalities that promote PI3K pathway activation. Interestingly, PIK3CA mutant lines were found to be statistically more sensitive than PIK3CA wild-type lines. However, equivalent sensitivity was observed between cells bearing a functional *PTEN* gene versus cells with phosphatase inactivating mutations or deletions. Identical observations were made for the pan-class I PI3K inhibitor GDC-0941, in an analysis restricted to a panel of 54 breast cancer lines (38). However, another study conducted with different PI3K inhibitors carried out in a panel of 39 lines from 9 different lineages did not show enhanced activity in either PIK3CA or PTEN mutant lines (39). These conflicting data might reflect the fact that, in the latter study, only a small number of lines for each lineage and genetic alteration were analyzed, with a strong imbalance in the representation of each characteristic. Moreover, evidences for an important function for p110β in PTEN-null cell and tumor models have been reported (40, 41). BKM120 is slightly less potent on p110β and the concentration used to establish the sensitivity profile (0.8 μmol/L) might have been insufficient to completely inhibit this isoform in our study.

Overall, pharmacologic inhibition of PI3K shows that: (i) a PIK3CA mutation is certainly not identical to a PTEN mutation/deletion in terms of PI3K addiction and (ii) PTEN mutant or deleted tumors might have addiction to other pathways for proliferation and survival. Understanding what these pathways would be could provide insightful information on which combination partners could be used to complement the efficacy of PI3K inhibitors. Although PIK3CA mutant tumors seemed to be more sensitive to PI3K inhibitors, one cannot conclude that all PIK3CA mutant tumors will respond to them. For instance, the cooccurrence of KRAS activating mutations dramatically reduces the sensitivity to NVP-BKM120. One explanation to this phenomenon is that pathways often converge into similar and important downstream key effectors, and efficacy is dependent upon silencing of all critical inputs to such downstream node. This was recently elegantly illustrated in KRAS mutant/PIK3CA mutant colorectal cancer models, in which efficacy could be achieved only when cyclin D1 levels could be reduced by cotreatment with MEK and Akt inhibitors (42). Similarly, apoptotic events in the HCT116 lines could be detected only when NVP-BKM120 was combined with the MEK inhibitor AZD6244, and these effects translated in strong enhanced *in vivo* antitumor activity.

Target modulation and good pharmacokinetic and pharmacodynamic correlation was achieved with NVP-BKM120 in tumor-bearing mice. Significant and dose-dependent antitumor activity was observed at dose levels sufficient to shut down the PI3K pathway, showing the strong relationship between compound concentration, pathway inhibition and efficacy. Suboptimal dose of NVP-BKM120 was enough to strongly enhance the antitumor activity of standard of care (cytotoxic or targeted agents) in various cancer types such as prostate (with Taxotere), HER2-amplified breast cancer, or gastric cancer (with Herceptin/trastuzumab) and GBM (with temozolomide). The fact that enhanced activity was also observed *in vivo* against KRAS mutant HCT116 tumors when BKM120 was combined with the MEK inhibitor AZD6244 and opens new opportunities in indications with high and unmet medical need, in which KRAS is frequently mutated (such as pancreatic cancers), but confirmatory studies are warranted to test and eventually validate this paradigm in the relevant preclinical models.

As found with other PI3K inhibitors (22, 43), NVP-BKM120 possesses strong antiangiogenic activity. Hence, highly angiogenic tumors could be very sensitive to the compound. NVP-BKM120 could, therefore, be used efficiently as second line treatment upon failure of approved antiangiogenic drugs such as sutent, or sorafenib, in the case of metastatic renal cell carcinoma. Of interest is the fact that NVP-BKM120 possesses excellent brain penetration, hence, there is the possibility to treat advanced nonresectable highly angiogenic GBM, mostly in combination with temozolomide-based therapies.

>In conclusion, we have identified NVP-BKM120 as a selective pan-class I PI3K inhibitor. This compound possesses excellent drug-like properties that have allowed its selection for full clinical development. NVP-BKM120 is currently in phase II trials, in parallel with our dual PI3K/mTOR inhibitor NVP-BEZ325. The outcome of these studies is eagerly awaited, as they will be of primary importance in understanding the clinical relevance of PI3K or dual PI3K/mTOR inhibition in different cancer indications.

Disclosure of Potential Conflicts of Interest

S.-M. Maira, S. Pecchi, A. Huang, M. Burger, M. Knapp, D. Sterker, C. Schnell, D. Guthy, T. Nagel, M. Wiesmann, S. Brachmann, C. Fritsch, P. Chène, K. Shoemaker, A.D. Pover, D. Menezes, G. Martiny-Baron, D. Fabbro, C.L. Wilson, R. Schlegel, F. Hofmann, W.R. Sellers, and C.F. Voliva

are Novartis employees. M. Dorsch and C. Garcia-Echeverria are Sanofi-Aventis employees.

Acknowledgments

The authors thank Marc Hattenberger, Fabian Stauffer, Sandra Mollé, Laurent Laborde, and Juliane Vaxelaire for excellent technical assistance.

The costs of publication of this article were defrayed in part by the payment of page charges. This article must therefore be hereby marked *advertisement* in accordance with 18 U.S.C. Section 1734 solely to indicate this fact.

Received July 8, 2011; revised October 17, 2011; accepted November 17, 2011; published OnlineFirst December 21, 2011.

References

1. Hawkins PT, Anderson KE, Davidson K, Stephens LR. Signalling through Class I PI3Ks in mammalian cells. Biochem Soc Trans 2006;34:647–62.
2. Zhao L, Vogt PK. Class I PI3K in oncogenic cellular transformation. Oncogene 2008;27:5486–96.
3. Yuan TL, Cantley LC. PI3K pathway alterations in cancer: variations on a theme. Oncogene 2008;27:5497–510.
4. Lee-Hoeflich ST, Crocker L, Yao E, Pham T, Munroe X, Hoeflich KP, et al. A central role for HER3 in HER2-amplified breast cancer: implications for targeted therapy. Cancer Res 2008;68: 5878–87.
5. Samuels Y, Wang Z, Bardelli A, Silliman N, Ptak J, Szabo S, et al. High frequency of mutations of the PIK3CA gene in human cancers. Science 2004;304:554.
6. Carpten JD, Faber AL, Horn C, Donoho GP, Briggs SL, Robbins CM, et al. A transforming mutation in the pleckstrin homology domain of AKT1 in cancer. Nature 2007;448:439–44.
7. Markman B, Dienstmann R, Tabernero J. Targeting the PI3K/Akt/mTOR pathway-beyond rapalogs. Oncotarget 2010;1:530–43.
8. Maira SM, Stauffer F, Brueggen J, Furet P, Schnell C, Fritsch C, et al. Identification and characterization of NVP-BEZ235, a new orally available dual phosphatidylinositol 3-kinase/mammalian target of rapamycin inhibitor with potent *in vivo* antitumor activity. Mol Cancer Ther 2008;7:1851–63.
9. Fayard E, Xue G, Parcellier A, Bozulic L, Hemmings BA. Protein kinase B (PKB/Akt), a key mediator of the PI3K signaling pathway. Curr Top Microbiol Immunol 2010;346:31–56.
10. Carracedo A, Lorente M, Egia A, Blazquez C, Garcia S, Giroux V, et al. The stress-regulated protein p8 mediates cannabinoid-induced apoptosis of tumor cells. Cancer Cell 2006;9:301–12.
11. Courtney KD, Corcoran RB, Engelman JA. The PI3K pathway as drug target in human cancer. J Clin Oncol 2010;28:1075–83.
12. van der Heijden MS, Bernards R. Inhibition of the PI3K pathway: hope we can believe in? Clin Cancer Res 2010;16:3094–9.
13. Garcia-Echeverria C, Pearson MA, Marti A, Meyer T, Mestan J, Zimmermann J, et al. *In vivo* antitumor activity of NVP-AEW541-A novel, potent, and selective inhibitor of the IGF-IR kinase. Cancer Cell 2004;5:231–9.
14. Fuchikami K, Togame H, Sagara A, Satoh T, Gantner F, Bacon KB, et al. A versatile high-throughput screen for inhibitors of lipid kinase activity: development of an immobilized phospholipid plate assay for phosphoinositide 3-kinase gamma. J Biomol Screen 2002;7: 441–50.
15. Palmer T. Undersanding enzymes. 3rd ed. Chichester, England: Ellis Horwood Limited; 1991.
16. Morgenstern JP, Land H. Advanced mammalian gene transfer: high titre retroviral vectors with multiple drug selection markers and a complementary helper-free packaging cell line. Nucleic Acids Res 1990;18:3587–96.
17. Zhao JJ, Liu Z, Wang L, Shin E, Loda MF, Roberts TM. The oncogenic properties of mutant p110alpha and p110beta phosphatidylinositol 3-kinases in human mammary epithelial cells. Proc Natl Acad Sci U S A 2005;102:18443–8.
18. Zhang H, Cicchetti G, Onda H, Koon HB, Asrican K, Bajraszewski N, et al. Loss of Tsc1/Tsc2 activates mTOR and disrupts PI3K-Akt signaling through downregulation of PDGFR. J Clin Invest 2003;112: 1223–33.
19. Brachmann S, Hofmann I, Schnell C, Fritsch C, Wee S, Lane H, et al., Specific apoptosis induction by the dual PI3K/mTOR inhibitor NVP-BEZ235 in HER2 amplified and PIK3CA mutant breast cancer cells. Proc Natl Acad Sci U S A 2009;106:22299–307.
20. van OJ, Calonder C, Rechsteiner D, Ehrat M, Mestan J, Fabbro D, et al. Tracing pathway activities with kinase inhibitors and reverse phase protein arrays. Proteomics Clin Appl 2009;3:412–22.
21. Clarke R. Issues in experimental design and endpoint analysis in the study of experimental cytotoxic agents *in vivo* in breast cancer and other models. Breast Cancer Res Treat 1997;46:255–78.
22. Schnell CR, Stauffer F, Allegrini PR, O'Reilly T, McSheehy PM, Dartois C, et al. Effects of the dual phosphatidylinositol 3-kinase/mammalian target of rapamycin inhibitor NVP-BEZ235 on the tumor vasculature: implications for clinical imaging. Cancer Res 2008;68: 6598–607.
23. Sutherlin DP, Sampath D, Berry M, Castanedo G, Chang Z, Chuckowree I, et al. Discovery of (thienopyrimidin-2-yl)aminopyrimidines as potent, selective, and orally available pan-PI3-kinase and dual pan-PI3-kinase/mTOR inhibitors for the treatment of cancer. J Med Chem 2010;53:1086–97.
24. Walker EH, Perisic O, Ried C, Stephens L, Williams RL. Structural insights into phosphoinositide 3-kinase catalysis and signalling. Nature 1999;402:313–20.
25. Walker EH, Pacold ME, Perisic O, Stephens L, Hawkins PT, Wymann MP, et al. Structural determinants of phosphoinositide 3-kinase inhibition by wortmannin, LY294002, quercetin, myricetin, and staurosporine. Mol Cell 2000;6:909–19.
26. Liu P, Cheng H, Roberts TM, Zhao JJ. Targeting the phosphoinositide 3-kinase pathway in cancer. Nat Rev Drug Discov 2009;8:627–44.
27. Chresta CM, Davies BR, Hickson I, Harding T, Cosulich S, Critchlow SE, et al. AZD8055 is a potent, selective, and orally bioavailable ATP-competitive mammalian target of rapamycin kinase inhibitor with *in vitro* and *in vivo* antitumor activity. Cancer Res 2010;70: 288–98.
28. Engelman JA. Targeting PI3K signalling in cancer: opportunities, challenges and limitations. Nat Rev Cancer 2009;9:550–62.
29. Yaguchi S, Fukui Y, Koshimizu I, Yoshimi H, Matsuno T, Gouda H, et al. Antitumor activity of ZSTK474, a new phosphatidylinositol 3-kinase inhibitor. J Natl Cancer Inst 2006;98:545–56.
30. Engelman JA, Chen L, Tan X, Crosby K, Guimaraes AR, Upadhyay R, et al. Effective use of PI3K and MEK inhibitors to treat mutant Kras G12D and PIK3CA H1047R murine lung cancers. Nat Med 2008;14: 1351–6.
31. Chandarlapaty S, Sawai A, Scaltriti M, Rodrik-Outmezguine V, Grbovic-Huezo O, Serra V, et al. AKT inhibition relieves feedback suppression of receptor tyrosine kinase expression and activity. Cancer Cell 2011;19:58–71.
32. Serra V, Scaltriti M, Prudkin L, Eichhorn PJ, Ibrahim YH, Chandarlapaty S, et al. PI3K inhibition results in enhanced HER signaling and acquired ERK dependency in HER2-overexpressing breast cancer. Oncogene 2011;30:2547–57.
33. Chakrabarty A, Sanchez V, Kuba MG, Rinehart C, Arteaga CL. Breast Cancer Special Feature: Feedback upregulation of HER3 (ErbB3) expression and activity attenuates antitumor effect of PI3K inhibitors. Proc Natl Acad Sci U S A. 2011 Feb 28. [Epub ahead of print].
34. Garrett JT, Olivares MG, Rinehart C, Granja-Ingram ND, Sanchez V, Chakrabarty A, et al. Transcriptional and posttranslational up-

regulation of HER3 (ErbB3) compensates for inhibition of the HER2 tyrosine kinase. Proc Natl Acad Sci U S A 2011;108:5021–6.
35. Graupera M, Guillermet-Guibert J, Foukas LC, Phng LK, Cain RJ, Salpekar A, et al. Angiogenesis selectively requires the p110alpha isoform of PI3K to control endothelial cell migration. Nature 2008;453:662–6.
36. Yuan TL, Choi HS, Matsui A, Benes C, Lifshits E, Luo J, et al. Class 1A PI3K regulates vessel integrity during development and tumorigenesis. Proc Natl Acad Sci U S A 2008;105:9739–44.
37. Burger MT, Pecchi S, Wagman A, Ni Z-J, Knapp M, Hendrickson T, et al. Identification of NVP-BKM120 as a potent, selective, orally bioavailable class I PI3 Kinase inhibitor for treating cancer. ACS Med Chem Lett 2011;2:774–9.
38. O'Brien C, Wallin JJ, Sampath D, GuhaThakurta D, Savage H, Punnoose EA, et al. Predictive biomarkers of sensitivity to the phosphatidylinositol 3′ kinase inhibitor GDC-0941 in breast cancer preclinical models. Clin Cancer Res 2010;16:3670–83.
39. Dan S, Okamura M, Seki M, Yamazaki K, Sugita H, Okui M, et al. Correlating phosphatidylinositol 3-kinase inhibitor efficacy with signaling pathway status: in silico and biological evaluations. Cancer Res 2010;70:4982–94.
40. Wee S, Wiederschain D, Maira SM, Loo A, Miller C, deBeaumont R, et al. PTEN-deficient cancers depend on PIK3CB. Proceedings of the National Academy of Sciences 2008;105:13057–62.
41. Jia S, Liu Z, Zhang S, Liu P, Zhang L, Lee SH, et al. Essential roles of PI(3)K-p110β in cell growth, metabolism and tumorigenesis. Nature 2008;454:776–9.
42. Halilovic E, She QB, Ye Q, Pagliarini R, Sellers WR, Solit DB, et al. PIK3CA mutation uncouples tumor growth and cyclin D1 regulation from MEK/ERK and mutant KRAS signaling. Cancer Res 2010;70:6804–14.
43. Kong D, Okamura M, Yoshimi H, Yamori T. Antiangiogenic effect of ZSTK474, a novel phosphatidylinositol 3-kinase inhibitor. Eur J Cancer 2009;45:857–65.